chical and interpolatory higher-order vector basis functions for finite element method and method of moments, 6th International Workshop on Finite Elements for Microwave Engineering, Antennas, Circuits and Devices—Book of Abstracts, Chios, Greece, 2002, p. 65.
8. E. Jorgensen, J.L. Volakis, P. Meincke, and O. Breinbjerg, Higher order hierarchical Legendre basis functions for iterative integral equation solvers with curvilinear surface modeling, 2002 IEEE Antennas Propagat Soc Int Symp Dig, San Antonio, TX, 2002, pp. IV.618–621.
9. B.M. Notaros and B.D. Popovic, Large-domain integral-equation method for analysis of general 3D electromagnetic structures, IEE Proceedings—Microwaves, Antennas and Propagation 145 (1998), 491–495.
10. M.M. Ilic and B.M. Notaros, Computation of 3-D electromagnetic cavity resonances using hexahedral vector finite elements with hierarchical polynomial basis functions, 2002 IEEE Antennas Propagat Soc Int Symp Dig, San Antonio, TX, 2002, pp. IV.682–685.
11. M. Abramowitz and C.A. Stegun (Eds.), Handbook of Mathematical Formulas, Graphs and Mathematical Tables, Ch. 22 Orthogonal Polynomials, New York-Dover, 1972, pp. 771–802.
12. M. Djordjevic and B.M. Notaros, Highly efficient large-domain moment-method analysis and CAD of radio-frequency antennas mounted on or situated in vehicles, Fall 2000 IEEE Vehicular Technology Conference Digest, Boston, MA, 2000, pp. 2373–2377.

LEAKY AND SURFACE WAVES IN MULTILAYERED LATERALLY-SHIELDED MICROSTRIP TRANSMISSION LINES

J. L. Gómez Tornero and A. Álvarez Melcón
Technical University of Cartagena
Campus Muralla del Mar s/n, 30202 Spain

Received 19 October 2002

ABSTRACT: *In this paper the leakage effects in open laterally-shielded multilayered microstrip transmission lines are investigated. Potential solutions are often reported to be difficult to find, since they are located in the complex propagating factor plane. To overcome this problem, a novel iterative algorithm is implemented to relate the solutions in the real axis of closed transmission lines with their corresponding complex open structure modes. The problem of modeling the leaky behavior of the open top wall is introduced, and a mathematical and physical explanation of the solutions is proposed. The advantage of this new technique is that it allows us to easily track the leaky solutions to their final location in the complex plane. Results are presented, including the field and power patterns associated to leaky waves, showing that the derived technique is indeed effective for the study of the complex modes excited in this type of structures.* © 2003 Wiley Periodicals, Inc. Microwave Opt Technol Lett 37: 88–93, 2003; Published online in Wiley InterScience (www.interscience.wiley.com). DOI 10.1002/mop.10832

Key words: *antennas; leaky waves; microstrip structures; numerical methods; integral equation*

1. INTRODUCTION

The leaky modes excited in open microstrip-like structures have been studied in the past by many researchers [1–13]. This radiation mechanism can be undesirable for printed-circuit applications, since it can cause interference and thus deteriorate the system performance. On the contrary, this radiation mechanism can be used in the design of leaky wave antennas [5, 11–13]. In any case, it is always convenient to control this leakage effect.

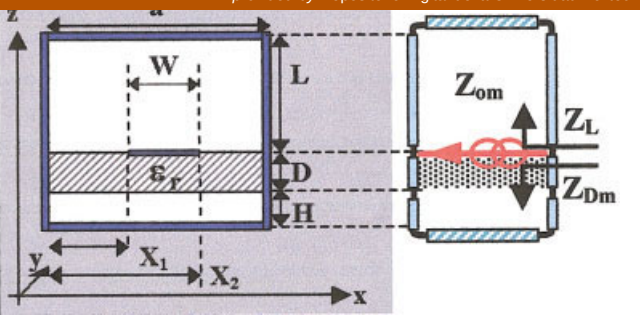

Figure 1 Cross section of the structure and equivalent network. [Color figure can be viewed in the online issue, which is available at www.interscience.wiley.com.]

The properties of the proposed solutions for microstrip configurations have also been mentioned in many papers, including the apparently growing amplitude behavior along the stratification axis [9]. However, how to mathematically treat this situation in order to retrieve the field pattern associated with leaky wave solutions is not easily found. The field associated to a leaky wave mode is computed in [6], but only over the metal strip, and no details are given as to how the field in the cross section can be evaluated. In addition, in [11–13] the field pattern is computed, but the leaky wave antenna is built using an empty waveguide with no dielectrics or printed metal strips. In the structure we propose, a suspended dielectric substrate is used in order to obtain a high gain behavior following similar ideas as those presented in [5].

Searching the complex poles of the leaky waves is also an interesting subject [8–10]. This is usually a complex task, since a search procedure must be implemented in a 2D complex plane. Yet, simple and efficient search strategies, which can be used to track the location of the complex leaky modes, are not generally found. For instance, in [10], the complex poles are found by taking as initial point in the search algorithm the quasi-static asymptotic location of the solutions at low frequency [8]. In addition to these iterative strategies, graphical procedures to approximately locate the complex leaky wave poles have also been derived [9].

Also, although many investigations have been conducted for basic printed lines [1–10], the same is not generally true for laterally shielded configurations. In all previous works, the infinite nature of the dielectric substrates yields to continuous wavenumbers in the spectral domain. For the shielded version, however, the discrete nature of the wavenumber must be carefully treated.

In this paper, we propose to study for the first time the leaky effects of a laterally shielded suspended microstrip line (Fig. 1). In addition to the basic formulation, we propose a novel technique which can be used to easily track the leaky modes as they move to the complex plane. This is essentially achieved by relating the leaky wave modes of the open transmission line with the real propagating waves of the closed counterpart. Also, the technique implemented can treat the growing behavior of the modes along the stratification axis, and this has allowed to obtain for the first time the field and power density distributions associated with these leaky wave modes.

The studied structure and the method used are presented in section 2. The modes in a closed transmission line, what we call the dielectric-bounded and the dielectric-leaky regimes, are obtained for a given example and properties of both are presented. The real modes of the closed structure will then be used in the novel search procedure to find the complex leaky wave solutions of the open structure. This novel search procedure for the complex

leaky solutions is presented in three steps. First, the mathematical formalism of the leaky functions is presented, leading to the definition of the required propagating factors of the structure. In the second step, the method derived to use the real solutions of the closed transmission line as a good initial point for the complex search of leaky modes is explained. In the last step, the procedure to change the top wall's boundary conditions from those of a closed transmission line to those of the open structure is showed.

Using this search procedure, the leaky waves of a typical structure are investigated in section 3 under three different physical situations, namely, the perfectly matched case, the accumulative match case, and the fundamental mode-matched case. In this section, the differences and problems in all these three situations will be stressed. The final results for the geometry under investigation are presented in section 4, including the 2D power density distribution plots associated with each physical wave propagating in the structure.

2. BASIC THEORY

In Figure 1, a laterally-shielded suspended microstrip line is shown. This structure can be analyzed with or without the top metal wall. The method used for this analysis is the integral equation. The Green's functions of an infinite wire inside a parallel plate wave guide (PPW) are expressed in terms of the modal expansion functions of this PPW, but modified to allow for a propagating factor in the longitudinal y axis.

This formulation leads to a set of equivalent transmission line networks in the stratification z axis [14] (see Fig. 1). The method of moments (MoM) is used to express the current distribution on the metal strip, and the electric field integral equation (EFIE) is imposed so that the transverse electric field will be zero on the metal discontinuity. As a result, a homogeneous system of linear equation is obtained Eq. (1), in which the α coefficients of the current basis functions can be solved:

$$[P] \cdot [\alpha] = 0 \tag{1}$$

In order to ensure a non-trivial solution, the determinant of the matrix P must be equal to zero. This determinant is a complex function that depends on the unknown variable K_y, which stands for the propagating factor in the longitudinal y axis. Therefore, the zeros of that function must be found for each solution. In Figure 2, an example for the closed structure is shown in which seven zeros

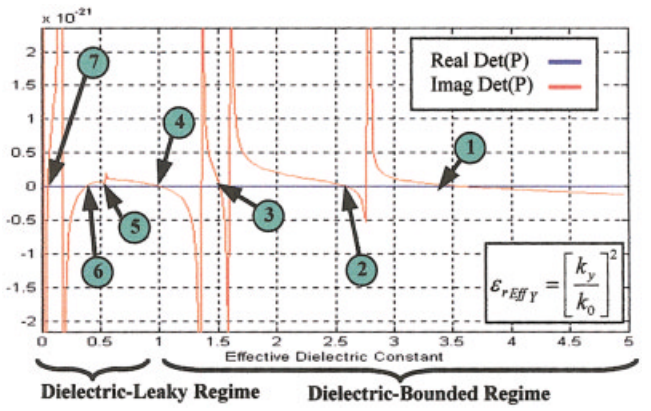

Figure 2 Modes and regimes for the closed transmission line. [Color figure can be viewed in the online issue, which is available at www.interscience.wiley.com.]

TABLE 1 Limits Between Regimes for Closed Transmission Line

Regime	β_y Limits	
Dielectric-Bounded	$\left[\sqrt{K_o^2 - \left(M_o \frac{\pi}{a}\right)^2},\ \sqrt{K_o^2 \varepsilon_r - \left(M_o \frac{\pi}{a}\right)^2}\right]$	(3)
Dielectric-Leaky	$\left[0,\ \sqrt{K_o^2 - \left(M_o \frac{\pi}{a}\right)^2}\right]$	(4)

are found, corresponding to the seven propagation modes of the transmission line for a given frequency.

For a lossless closed transmission line, the zeros can be found in the real $K_y = \beta_y$ axis. These real solutions can be divided in two different propagation regimes. In the dielectric-bounded regime the energy is confined inside the dielectric slab, while in the dielectric-leaky regime the energy propagates in both dielectric and air media. The limit between these two regimes can be obtained from the analysis of the propagating factor in the z axis, K_{zm}:

$$K_{zm}^{VACUUM} = \sqrt{K_0^2 - \left(m \frac{\pi}{a}\right)^2 - K_y^2}\ \ m = 0, 1, 2 \ldots \tag{2}$$

From Eq. (2), the limits in the real $K_y = \beta_y$ axis are written in Table 1, where M_o stands for the first excited modal function which propagates energy in the structure.

For the example of Figure 2 (with $\varepsilon_r = 5$), the four first modes belong to the dielectric-bounded regime, while the last three are dielectric-leaky modes. Once this distinction has been made, the open structure modes can be studied by trying to relate them with their corresponding modes of the closed transmission line.

If the top metal wall is removed, the modes of the original closed structure will be modified to account for the new boundary conditions, and two different regimes for the open case may exist. The surface waves are those modes in which the energy remains confined in the dielectric slab despite the top aperture. On the contrary, for the leaky waves, the energy can escape out from the structure, leading to a leakage of energy as the mode propagates along the y axis. This leakage effect causes the K_y solution of the leaky waves to be complex, with a negative imaginary part that accounts for the radiation losses, given by

$$K_y = \beta_y - j\alpha_y. \tag{5}$$

The search for these complex zeros is quite difficult, since a 2D search algorithm with a good initial point is needed, and the zeros can be closed to the poles of the function. In order to overcome this problem, we propose a novel technique based on relating the solutions between the closed and open scenarios.

The relation between the two structures, however, can not be done in a straightforward manner. The set of modal functions used to express the total field of a given solution has a propagating factor in the z direction for vacuum K_{zm}, which can be related with K_y according to expression (2). For the closed structure, as K_y is real, the modal functions will have a z behavior either above or below cut-off. On the contrary, for a leaky mode, assuming the complex K_y solution, the mathematical formalism leads to a complex modal K_{zm} with a positive imaginary part (see Fig. 3). As can be seen in Figure 3, these two types of solutions are quite different. However, the modal propagating factor K_{zm} can be conjugated, so the modal function below cut-off now has a positive imaginary

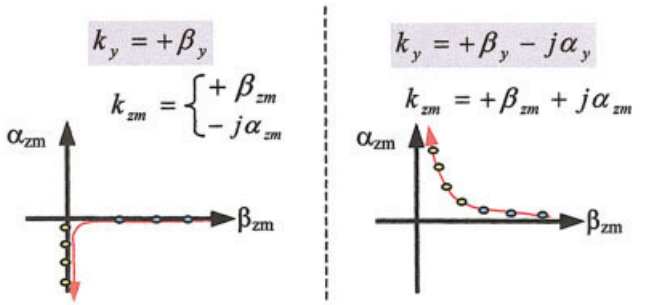

Figure 3 Modal propagating factors for closed and leaky modes. [Color figure can be viewed in the online issue, which is available at www.interscience.wiley.com.]

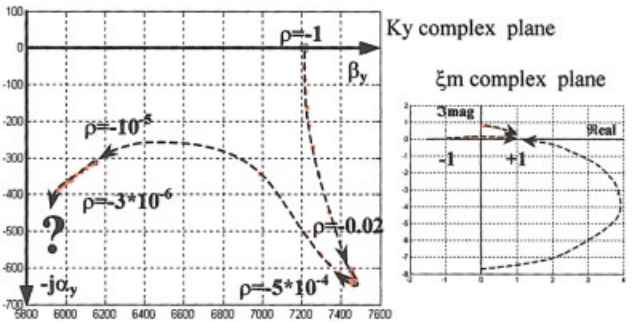

Figure 5 All modal functions perfectly matched strategy for mode 5. [Color figure can be viewed in the online issue, which is available at www.interscience.wiley.com.]

K_{zm}. Fortunately, these changes in the field expressions can serve as a solution for the closed structure due to their symmetry properties, and this solution can be used as an initial point for the search of leaky waves.

The initial point and the final situation can be seen in Figure 4. The main difference between them is in the boundary conditions of the top wall. This is represented in this method by the equivalent modal top impedance Z_{Lm} which has to change from that of a metal wall to that of an open wall. A procedure must be chosen to move from one situation to another in a manner which allows us to relate the initial point in the real β_y axis with the final solution in the complex plane.

3. SEARCH STRATEGIES

The first strategy presented to enable the change from the closed transmission line to the open top wall structure assumes that this open aperture can be modeled by an ideal perfectly matched tap. The equivalent top impedance can be expressed as:

$$Z_{Lm} = Z_{0m} \cdot \xi_m, \tag{6}$$

where the new parameter ξ_m stands for the normalized equivalent modal top impedance. In this way it can be readily seen that the situation of a perfectly matched wall corresponds to ξ_m equal to $+1$ for all the modal functions. Using the reflection coefficient of the top wall ρ, ξ_m can be expressed as

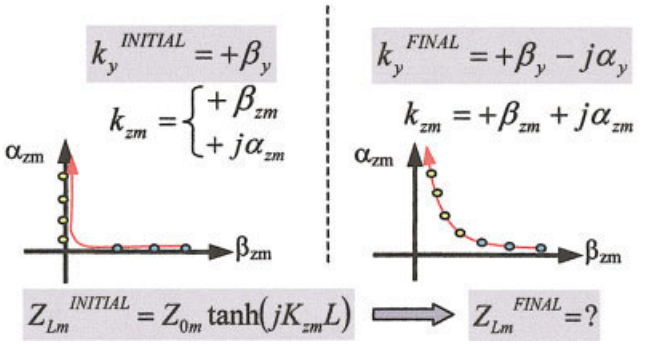

Figure 4 Initial and final situations in the leaky search. [Color figure can be viewed in the online issue, which is available at www.interscience.wiley.com.]

$$\xi_m = \frac{\dfrac{1+\rho}{1-\rho} + \tanh(jK_{zm}L)}{1 + \dfrac{1+\rho}{1-\rho}\tanh(jK_{zm}L)}. \tag{7}$$

This procedure consists in changing the boundary conditions of the top wall from $\rho^{INI} = -1$ to $\rho^{FINAL} = 0$ in several small steps. Then, at each step an efficient search routine will be able to find the final complex solution by starting from the initial point in the real β_y axis.

The first interesting result is that the leaky modes can only be found by starting from the dielectric-leaky regime of the closed structure (Fig. 2). Using the example of Figure 2, there are three dielectric-leaky modes, numbered 5, 6, and 7. In Figure 5, it can be observed that the complex path obtained as the reflection coefficient changes from the metal wall to the perfectly matched top aperture for mode number 5.

As expected, the K_y solution moves to the complex leaky plane, but unfortunately, when ρ gets very close to zero, the algorithm does not converge and the tracking is lost. This problem is due to the fact that for $\rho = 0$ all the modal functions must be perfectly matched to the aperture. In Figure 5 the movement of the modal functions in the complex ξ_m plane can also be seen. In the initial point from the dielectric-leaky mode of the closed structure, two modal functions were above cut-off in the vacuum, while the rest were below cut-off. In the ξ_m plane, the modal function above cut-off are mapped in the imaginary ξ_m axis, while the rest are very closed to -1, as can be obtained from the initial ξ_m (when $\rho = -1$):

$$\xi_m^{INI} = \tanh(jK_{zm}L) \tag{8}$$

The final situation in the ξ_m plane can be written as

$$\xi_m^{FINAL} = +1. \tag{9}$$

In this way, all the modal functions below cut-off have to move from $\xi_m \approx -1$ to $\xi_m = +1$. As ρ tends to zero, more modal functions will make this strong change for their boundary conditions in the ξm plane, and this will traduce into a strong change without convergence in the solution in the Ky complex plane.

To overcome the convergence difficulties, another strategy has been derived. In this case only a fixed amount of modal functions are going to be moved from the original boundary conditions of the top metal wall to the point $\xi_m = +1$ (that is, the aperture is matched only for these modal functions). The rest of the modal

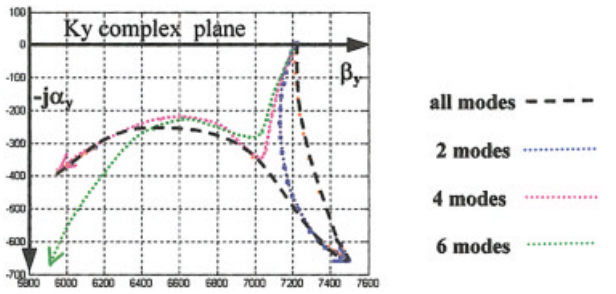

Figure 6 Accumulative matched modes technique for mode 5. [Color figure can be viewed in the online issue, which is available at www.interscience.wiley.com.]

functions will remain mismatched at the point $\xi_m = -1$. Since the number of matched modal functions increases in an accumulative way, complex solutions are found very closed to the curve obtained with the previous strategy, as shown in Figure 6.

In addition to the accumulative number of modes, a third strategy is proposed to model the top open wall in a simple manner. Instead of trying to match all the modal functions, or only a given amount of them, the top impedance can be matched to the characteristic impedance of only the dominant modal function of the PPW expansion. Again using the top reflection coefficient ρ, the top boundary impedance can be changed from a metal wall to that of the final matched impedance with the following expression:

$$Z_{TopWall}^{ITER} = Z_{o\ m=0}\,\frac{1+\rho^{ITER}}{1-\rho^{ITER}}, \tag{10}$$

where ρ^{ITER} is the reflection coefficient at each iteration. Therefore, the equivalent modal top impedance will change according to the following expression:

$$Z_{Lm} = Z_{om}\,\frac{Z_{TopWall} + Z_{om}\tanh(jKzmL)}{Z_{om} + Z_{TopWall}\tanh(jKzmL)} = Z_{om}\cdot\xi_m. \tag{11}$$

As can be seen, only the dominant modal function will be perfectly matched to the top wall in the last iteration, while the rest of the modal function will be mismatched accordingly.

Using this technique, a leaky wave complex solution is found from modes 5, 6, and 7. In Figure 7 the mode-5 leaky search is shown.

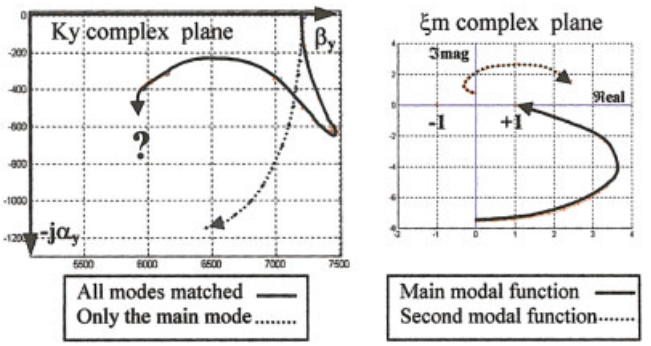

Figure 7 Main mode-matched technique for mode 5. [Color figure can be viewed in the online issue, which is available at www.interscience.wiley.com.]

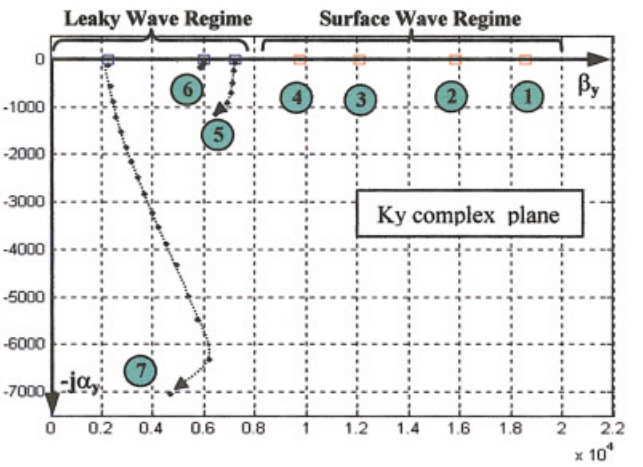

Figure 8 Final solutions for the top open structure. [Color figure can be viewed in the online issue, which is available at www.interscience.wiley.com.]

As it can be seen in the ξ_m plane, only the dominant modal function arrives at $\xi_m = +1$ with this technique, while the rest of the modal functions remain mismatched in the ξ_m complex plane.

Following this technique, the leaky wave complex solutions are found to match only the dominant modal function and, most importantly, are taken as the initial point of the real solution for the closed structure in the dielectric-leaky regime.

Moreover, the modes of the closed transmission line in the dielectric-bounded regime are confined in the dielectric slab without any modal function propagating in the vacuum. Using the leaky mathematical formalism, no complex solutions can be derived from these modes. In fact, these modes will not suffer much transformation when removing the top electric wall, and will stay in the real β_y axis, propagating inside the dielectric slab without leakage. Assuming a real solution $K_y = \beta_y$, the same mathematical formalism used for the closed structure can be formulated, but changing the top boundary condition from that of a metal wall to that of a perfectly matched wall. Because all the modal functions are below cut-off in the vacuum, in the ξ_m complex plane they are mapped very closed to $+1$. The movement to the final situation of perfect matching for all modal functions ($\xi_m = +1$) is very small, and therefore the solution changes very little, remaining in the real β_y axis.

4. FINAL RESULTS

Once the influence of removing the top wall has been studied, the final solutions in the complex K_y plane can be presented in Figure 8 for the example of Figure 2, where seven modes appeared for the closed structure.

The first four modes are surface waves, which come from the dielectric-bounded regime of the closed transmission line. The open wall has barely affected them, and the zeros will still stay in the real β_y axis. The power distribution of these modes can be obtained to check these "surface" natures.

In the first column of Figure 9, the longitudinal power flux is represented for the dielectric-bounded modes of the closed transmission line. When opening the top wall the fields are barely affected, and the longitudinal power pattern does not essentially change (see second column of Fig. 9). In the third column of Figure 9, the transverse power flux of the open structure is represented. For both the closed and open cases, this transverse average power is null, since all the energy is stored inside the dielectric

between the top and bottom magnetic walls of the dielectric slab and the side metal walls. These walls act as a combined magnetic-electric rectangular waveguide to propagate the energy along the y axis without any leakage.

The three last modes are leaky waves. They come from the dielectric-leaky regime of the closed structure, and are very dependent on the top and bottom metal walls. When the top wall is removed, they suffer a big change in their top boundary conditions, and the solution moves from the real β_y axis to the complex $K_y = \beta_y = j\alpha_y$ quadrant.

In the first column of Figure 10, the longitudinal power flux is displayed for the dielectric-leaky modes of the closed structure. It can be observed how the energy propagates in both dielectric and air media. The transverse average pointing vector for the shielded transmission line is not represented because it is null, due to the fact that all the transverse energy is stored between the metal walls.

The second column represents the same longitudinal pointing vector, in this case for the leaky wave of the open top wall case. How this longitudinal power density changes can be observed accordingly. In addition, the biggest change occurs in the transverse power flux distribution (third column), which now is not zero. There is a net power flux which escapes from the structure through the top aperture. In fact, the higher the intensity of this leakage of energy, the greater the absolute value of the radiation loss constant of the complex solution, as can be observed in Figure 8 for the leaky mode number 7.

5. CONCLUSION

Modes that can propagate in a microstrip-suspended laterally-shielded transmission line have been studied, with special emphasis on the leakage effects when the structure is not completely closed. The leaky modes search has been investigated under three different physical situations: all modes matched, an accumulative number of matched modes, and only the dominant mode matched.

The surface and leaky modes of the open structure can be related to the modes of the closed transmission line. This allows us to easily track the leaky modes to their final position on the complex plane, and also have a better understanding of the influence of the top aperture. The technique presented in this paper is useful, since it allows the radiation mechanisms of this type of structure to be studied for a given working frequency.

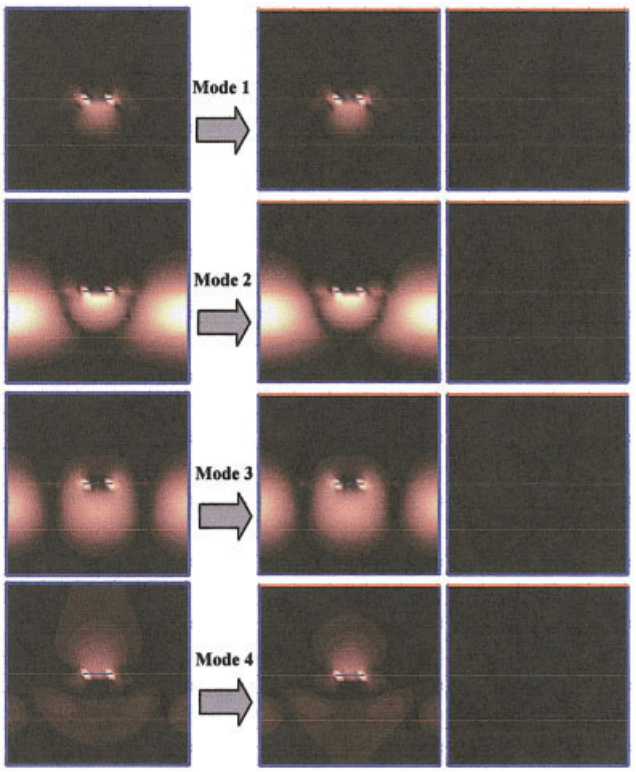

Figure 9 Power density for dielectric-bounded and surface modes. [Color figure can be viewed in the online issue, which is available at www.interscience.wiley.com.]

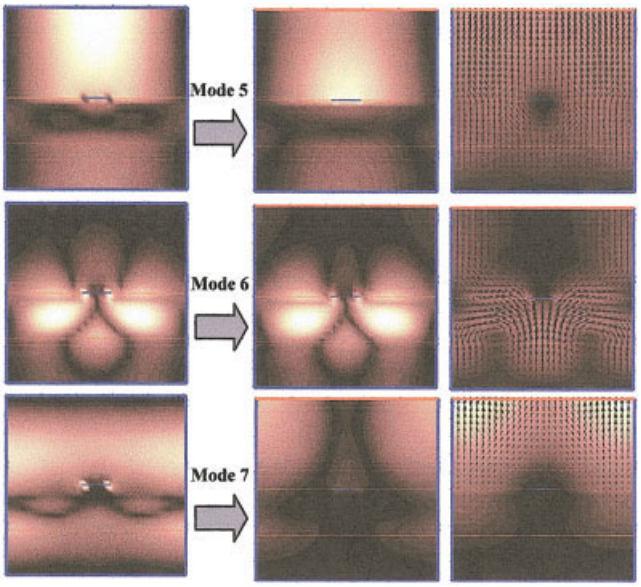

Figure 10 Power density for dielectric-leaky and leaky modes. [Color figure can be viewed in the online issue, which is available at www.interscience.wiley.com.]

REFERENCES

1. H. Ermert, Guided modes and radiation characteristics of covered microstrip lines, A.E.U. Band 30 (1976), 65–70.
2. A.A. Oliner and K.S. Lee, The nature of leakage from higher order modes on microstrip lines, IEEE Int Microwave Symp Dig 1986, Baltimore, MD, pp. 57–60.
3. A.A. Oliner, Leakage from higher modes on microstrip line with application to antennas, Radio Sci 22 (1987), 907–912.
4. K.A. Michalski and D. Zheng, On the leaky modes of open microstrip lines, Microwave Opt Technol Lett 2 (1989), 6–8.
5. D.R. Jackson, A.A. Oliner, A leaky-wave analysis of the high-gain printed antenna configuration, IEEE Trans Antennas Propagat 36 (1988).
6. L.O. McMillan, N.V. Shuley, and P.W. Davis, Leaky fields on microstrip, Progress In Electromagnetics Research, PIER 17 (1997), 323–337.
7. J.S. Bagby, C. Lee, D.P. Nyquist, and Y. Yuan, Identification of propagation regimes on integrated microstrip transmission lines, IEEE Trans MTT 41 (1993), 1887–1894.
8. M. Guglielmi and D.R. Jackson, Low-frequency location of the leaky-wave poles for a dielectric layer, IEEE Trans MTT 38 (1990), 1743–1746.
9. C.G. Hsu, R.F. Harrington, J.R. Mautz, and T.K. Sarkar, On the location of leaky wave poles for a grounded dielectric slab, IEEE Trans MTT 39 (1991), 346–349.
10. V. Galdi and I.M. Pinto, Efficient computation of leaky-wave poles for grounded inhomogeneus dielectric slab, IEEE Antennas and Propagation Conference, Davos, September 2000.
11. P. Lampariello, F. Frezza, H. Shigesawa, M. Tsuji, and A.A. Oliner, A versatile leaky-wave antenna based on stub-loaded rectangular

waveguide. Part I—Theory, IEEE Trans Antennas Propagat 46 (1998), 1032–1041.
12. P. Lampariello, F. Frezza, H. Shigesawa, M. Tsuji, and A.A. Oliner, A versatile leaky-wave antenna based on stub-loaded rectangular waveguide. Part II—Effects of flanges and finite stub length, IEEE Trans Antennas Propagat 46 (1998), 1042–1046.
13. P. Lampariello, F. Frezza, H. Shigesawa, M. Tsuji, and A.A. Oliner, A versatile leaky-wave antenna based on stub-loaded rectangular waveguide Part III—Comparison with measurements, IEEE Trans Antennas Propagat 46 (1998), 1047–1055.
14. Sheng-Gen Pan and Ingo Wolff, Scalarization of Dyadic Spectral Green's Functions and Network Formalism for Three-Dimensional Full-Wave Analysis of Planar Lines and Antennas. IEEE Trans Microwave Theory and Techniques 42 (1994), 2118–2127.

CIRCULARLY POLARIZED MICROSTRIP ANTENNA WITH A RECTANGULAR GROUND PLANE

Che-Wei Su and Kin-Lu Wong
Department of Electrical Engineering
National Sun Yat-Sen University
Kaohsiung 80424, Taiwan

Received 18 October 2002

ABSTRACT: *An experimental study of the nearly square circularly polarized microstrip antenna with a rectangular ground plane is presented. Results indicate that circular polarization characteristics of the nearly square microstrip antenna are greatly affected by the different side lengths of the rectangular ground plane. To compensate for this effect, the aspect ratio of the nearly square radiating patch should be increased when the aspect ratio of the ground plane increases. Details of the experimental results are presented.* © 2003 Wiley Periodicals, Inc. Microwave Opt Technol Lett 37: 93–95, 2003; Published online in Wiley InterScience (www.interscience.wiley.com). DOI 10.1002/mop.10833

Key words: *antennas; microstrip antennas; circularly polarized antennas*

1. INTRODUCTION

Circularly polarized microstrip antennas that have been studied usually have a square or circular ground plane, and the ground plane is symmetrically centered below the microstrip patch [1–3]. However, for practical applications, the antenna may be required to be mounted on a ground plane of non-square or non-circular shape. In this condition, the effects of such a ground plane (for example, a rectangular ground plane) on the circularly polarized microstrip antenna have not been analyzed, and related information is not available in the open literature.

In this paper, we present an experimental study of the nearly square circularly polarized microstrip antenna with a rectangular ground plane. The effects of different aspect ratios of the rectangular ground plane on the circular polarization (CP) characteristics of a nearly square microstrip antenna are analyzed, and the experimental results are presented.

2. ANTENNA GEOMETRY AND EXPERIMENTAL RESULTS

Figure 1 shows the geometry of the nearly square circularly polarized microstrip antenna. The nearly square radiating patch of dimensions $L \times W$ is printed on a grounded FR4 substrate of relative permittivity 4.4, thickness 1.6 mm, and size $A \times B$. The antenna is diagonally fed using a probe feed, with the feed point at a distance d away from the patch center.

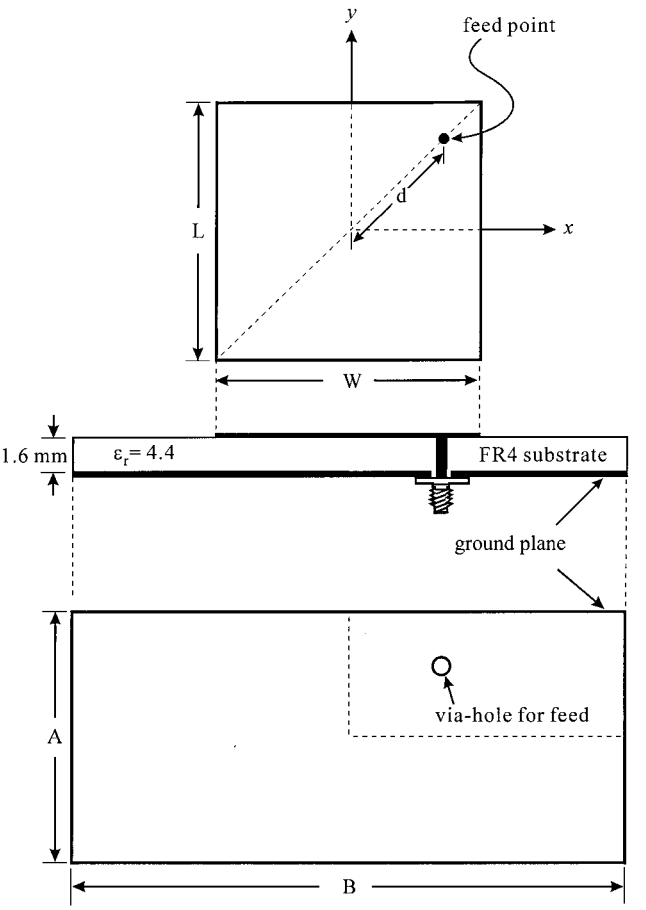

Figure 1 Geometry of the nearly square circularly polarized microstrip antenna with a rectangular ground plane

In this study, a reference antenna with a square ground plane ($A = B = 100$ mm) for CP radiation was first constructed and tested. For achieving global positioning system (GPS) applications at 1575 MHz, the dimensions of the nearly square radiating patch were chosen to be 45.8 mm (L) $\times$ 44.5 mm (W), with an aspect ratio (L/W) of 1.029. The measured input impedance on a Smith chart for the reference antenna is shown in Figure 2(a). The obtained impedance bandwidth (2:1 VSWR) is 62 MHz (1545–1607 MHz) and, as shown in Figure 3, the CP bandwidth (3-dB axial-ratio bandwidth) is 15 MHz (1566–1581 MHz), which covers 1575 MHz for GPS operation. The obtained CP performance is also listed in Table 1 for comparison.

Then, by decreasing the width A of the grounded FR4 substrate, many nearly square microstrip antennas with a rectangular ground plane were constructed and studied. Measured radiation characteristics are shown in Table 1 (see antennas 1 to 5 with $B = 100$ mm and $A = 80$, 70, 60, and 50 mm). The measured input impedance on a Smith chart for the antennas with $A = 70$ mm (antenna 3), 60 mm (antenna 4), and 50 mm (antenna 5) are also presented in Figure 2(b), (c), and (d), respectively.

It is first observed that, when A decreases and the aspect ratio of the nearly square radiating patch remains the same as that of the reference antenna, the CP radiation quickly degrades. For the case of $A = 70$ mm (aspect ratio (B/A) of the ground plane of about 1.43), the measured axial ratio is greater than 3 dB; that is, no CP